

## Article

# Median U-Turn Intersection Critical Parameter Research and Operational Performance Evaluation

Changxiang Zhao, Xuewen Liu \*, Tianhao Wu and Weiwei Zhang

School of Mechanical and Automotive Engineering, Shanghai University of Engineering Science, Shanghai 201620, China; changx962@126.com (C.Z.); wutianhao888@163.com (T.W.); weiweiz@smarter.com (W.Z.)  
\* Correspondence: xuewen2018@126.com

**Abstract:** As one of the unconventional intersection designs, the median U-turn (MUT) intersection design has been confirmed to have the potential to improve intersection efficiency and produce lower vehicle delays, and it has been widely applied to many urban networks. Most existing studies have successfully evaluated the operational performance of MUT intersections by analyzing the overall traffic flow, particularly for intersection delay and capacity. However, the impact of the critical parameters and behavior of individual vehicles in MUT intersection operations has not been adequately studied. These limitations cannot provide a complete and objective evaluation of MUT intersections. Therefore, a comprehensive cellular automata model is proposed to simulate vehicle dynamic variations, considering road channelization information and vehicle random movements. This model will be compared to the VISSIM model to validate rationality by using field data, and it shows a good agreement between the simulation results of both models. In addition, sensitive experiments reveal that properly adjusting the elements, including the separation distance, the proportion of left-turn vehicles, and green phase percentage, can improve the operation of MUT intersections to varying degrees. By appropriately improving intersection features and conducting reasonable evaluations, the overall performance and sustainability of the MUT intersections in Xi'an city can be enhanced. Finally, this paper offers a valuable guideline for the evaluation and modeling strategies of MUT intersections.

**Keywords:** median U-turn intersections; critical parameters; cellular automata model; VISSIM; operational performance



**Citation:** Zhao, C.; Liu, X.; Wu, T.; Zhang, W. Median U-Turn Intersection Critical Parameter Research and Operational Performance Evaluation. *Appl. Sci.* **2024**, *14*, 11445. <https://doi.org/10.3390/app142311445>

Received: 18 October 2024  
Revised: 29 November 2024  
Accepted: 4 December 2024  
Published: 9 December 2024



**Copyright:** © 2024 by the authors. Licensee MDPI, Basel, Switzerland. This article is an open access article distributed under the terms and conditions of the Creative Commons Attribution (CC BY) license (<https://creativecommons.org/licenses/by/4.0/>).

## 1. Introduction

As a key node of road networks, signalized intersections usually serve as the most important way to manage and control urban transportation and vehicle movements [1]. With the increase in vehicle ownership in urban areas, signalized intersections are becoming increasingly busy and congested [2]. Generally, the left-turn traffic within intersections is considered as one of the crucial factors that may cause traffic congestion [3], because it is a real possibility that left-turn traffic passing the intersections collides with the traffic from other directions [4,5]. The crossings of different vehicle movement trajectories within the intersections are called conflict points [6,7]. The existence of conflict points normally causes higher accident rates and severe casualties in the intersections [8]. Given the data from the National Highway Traffic Safety Administration (NHTSA) and Fatality Analysis and Reporting System (FARS), there are almost 9000 fatalities and about 1.5 million injuries caused by left-turn movements occurring annually in the United States [9]. Therefore, to ensure that intersections can operate more safely and efficiently, left-turn traffic should be regularized scientifically. In recent years, shifting and reorganizing the conflict points outside intersections to reduce their number has become a major concern in many unconventional intersection designs [10]. Among them, these unconventional intersection designs include median U-turns, restricted crossing U-turns (RCUTs), and displaced left-turns (DLTs). One

of the better-known and more widely used intersections is the median U-turn (MUT) intersection. The concept of the MUT intersection first emerged in the United States, particularly in Michigan, where it has been widely adopted. This innovative intersection is removing the direct left-turn movements of vehicles to accommodate indirect left-turn movements through median U-turns. It only allows the through traffic from major and minor roads to pass through the unclosed median. Figure 1 shows an example of a signalized MUT intersection in Michigan.

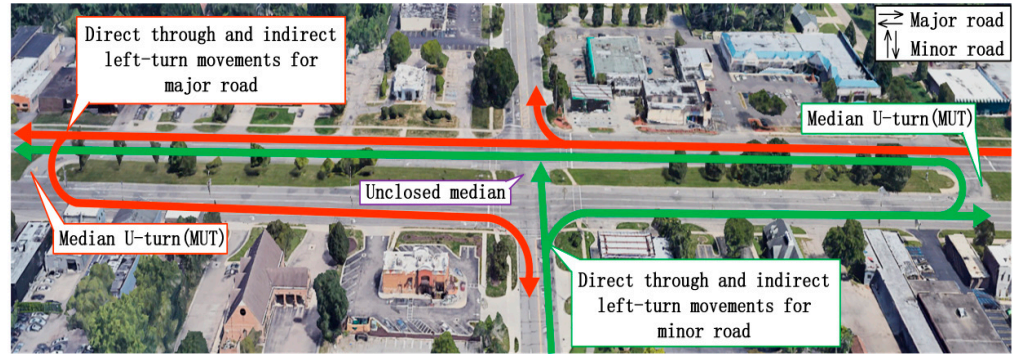


**Figure 1.** The operation of a signalized median U-turn (MUT) intersection in Michigan (adapted from Google Earth).

To some extent, the signalized MUT intersection is considered to have the potential to improve driving safety and reduce unnecessary delays for vehicles at intersections by decreasing the number of conflict points. It would be of considerable value to evaluate the safety benefits for traffic performance operation [11]. Figure 2 illustrates how an MUT intersection can effectively reduce the number of conflict points from 32 to 16.

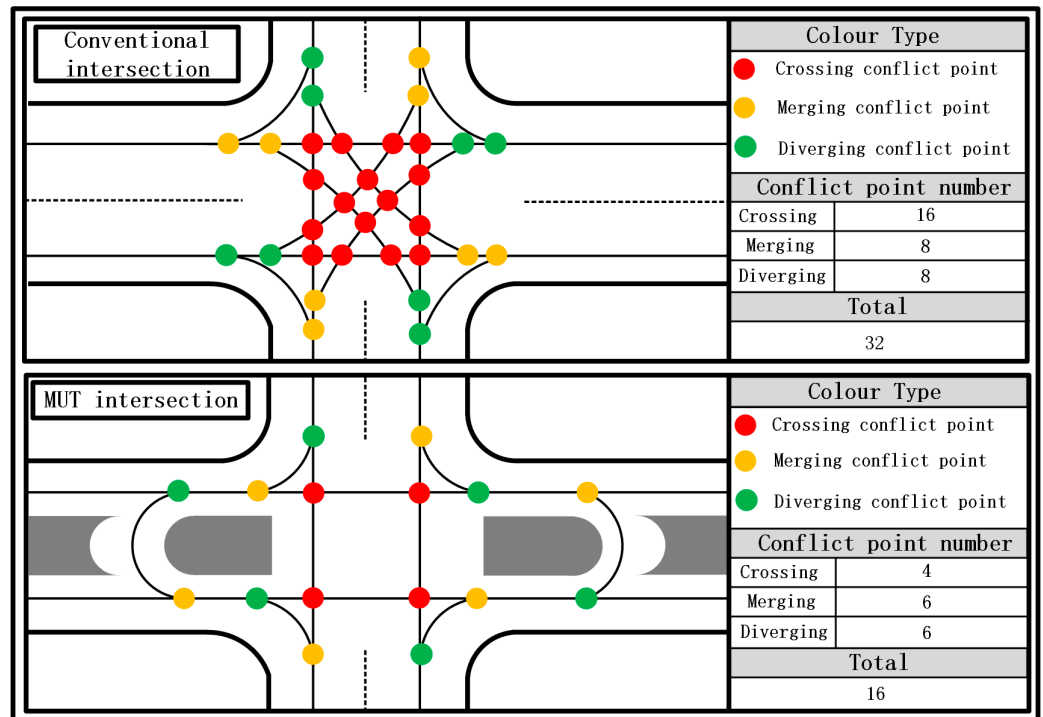


**Figure 2.** Conventional and media U-turn (MUT) intersection conflict points.

Relevant studies have confirmed that MUT intersections increase safety and reduce accidents because there is no opportunity for direct left-turns or head-on collisions. Compared with conventional intersections, the implements of MUT intersections are expected to

result in total crash reductions ranging from 20% to 50% [12,13]. Al-Omari et al. conducted a safety evaluation and concluded that MUT intersections can reduce head-on crashes by more than 80% and rear-end left-turn crashes by 48% [14]. Hummer and Reid used CORSIM to analyze the traffic performance of MUT intersections and found that the implementation of MUT intersections resulted in overall reductions in rear-end, angle, and sideswipe crashes by 17%, 96%, and 61%, respectively [15,16].

Although many studies have concluded that MUT intersections offer significant benefits to traffic capacity and efficiency, there are various areas that remain unexplored in studies of MUT intersections. Specifically, there is no widely accepted theory for calculating the critical parameters of MUT intersections, such as the distance between unclosed median and median U-turns (separation distance), or the gap and width of median U-turns. The following studies address these parameters. Firstly, in terms of the separation distance, Maryam et al. found that the separation distance is influenced by the number of conflicting driveways, median opening type, and the number of arterial lanes by evaluating median U-turn operations [17]. Pan Liu et al. analyzed how the separation distance impacts the safety performance of vehicles turning around via median U-turns [18]. Zhou et al. developed an operational model to determine the optimal location for median U-turns [19]. Secondly, in terms of the gap of median U-turns, related scholars conducted a driving simulation study and found significant differences in driving metrics across various median opening gaps [20]. Finally, in terms of the width of median U-turns, Jagannathan recommended different widths for various types of vehicles to improve the capacity of median U-turns [21]. On the whole, a significant gap in current studies is the integration of these parameters into a comprehensive assessment of overall MUT intersection performance. Most of them have failed to consider variations in traffic volumes, road features, and variable traffic conditions, which may result in inaccuracy and unreliable research findings. In order to better analyze the operational performance of MUT intersections, it is necessary to construct a reasonable model to characterize the actual variations in traffic flow based on diverse traffic volumes and road features.

This study fills a significant gap in the existing literature by integrating these critical parameters into a comprehensive assessment model for MUT intersections. Modeling and estimating the traffic movements and vehicle delays at MUT intersections are essential for evaluating intersection performance in complex traffic environments. The results of this research can assist transportation engineers and urban planners in designing safer and more efficient MUT intersections. Selecting appropriate modeling techniques is crucial to accurately reflect the dynamic operations of MUT intersections. Different traffic flow modeling techniques, including cellular automata, microscopic simulation models (e.g., VISSIM), and macroscopic traffic flow models, can be employed to simulate complicated traffic movements and delays at MUT intersections. Several studies have explored different approaches to modeling MUT intersections. Mane et al. developed a model of MUT intersections by using Synchro/SimTraffic (Version 7.0) traffic simulation software to obtain certain performance measures with specific conditions [22]. Al-Omari and his team used VISSIM models for MUT and restricted crossing U-turn (RCUT) intersections to assess the safety and operational aspects of these unconventional designs through a crash analysis, microscopic simulation, and driving simulation [23]. Liu et al. compared the performance of hook-turn (HT) and median U-turn intersections based on VISSIM simulations [24]. Pan Liu et al. proposed a calibrated VISSIM model to estimate the capacity more accurately by incorporating behavioral features of U-turning drivers, such as the priority rule, lane selection, and turning speed [25]. Arash et al. examined optimal distances between median U-turns and signalized intersections by inputting statistical data into the Aimsun (Version 8.3) traffic simulation software [26]. However, many of these studies have overlooked three aspects: (1) Existing vehicle input methods reflecting the randomness and uncertainty of traffic are still not objective. This is because the traffic state of MUT intersections has strong time-varying characteristics. Therefore, the vehicle random input models have to be selected reasonably. (2) There are no detailed regulations and divisions of lane-changing rules for vehicles at intersections. Vehicles must

change lanes to the corresponding lane and wait for the traffic light signal before passing the intersections. Then, vehicles with a left-turn demand have to turn around and merge into the opposite lanes. Therefore, this process must be reasonably refined to ensure the accuracy of the simulation. (3) One rarely considers the behavior of individual vehicles and drivers from a microperspective, including acceleration, deceleration, lane changing, and following distance, etc. These factors can significantly affect traffic flow and delays at MUT intersections, considering these factors can lead to more precise simulations and improve the accuracy of performance evaluations for MUT intersections.

In this paper, we developed a cellular automata model to simulate the overall operation of MUT intersections, taking into account their critical parameters and vehicle motion rules. The field data collected at a certain MUT intersection in Xi'an, China, were input into the proposed cellular automata model to obtain the simulation results. Furthermore, the accuracy and practicality of the cellular automata model will be validated by comparing them with the VISSIM model under certain conditions. The relevant findings are expected to offer valuable recommendations for evaluating MUT intersections and modeling strategies in complex traffic environments. The findings of this study are expected to contribute to the improvement of traffic management strategies and intersection design, offering insights for policymakers and engineers working to enhance road safety, and reduce traffic congestion. The main procedure for this study is shown in Figure 3.

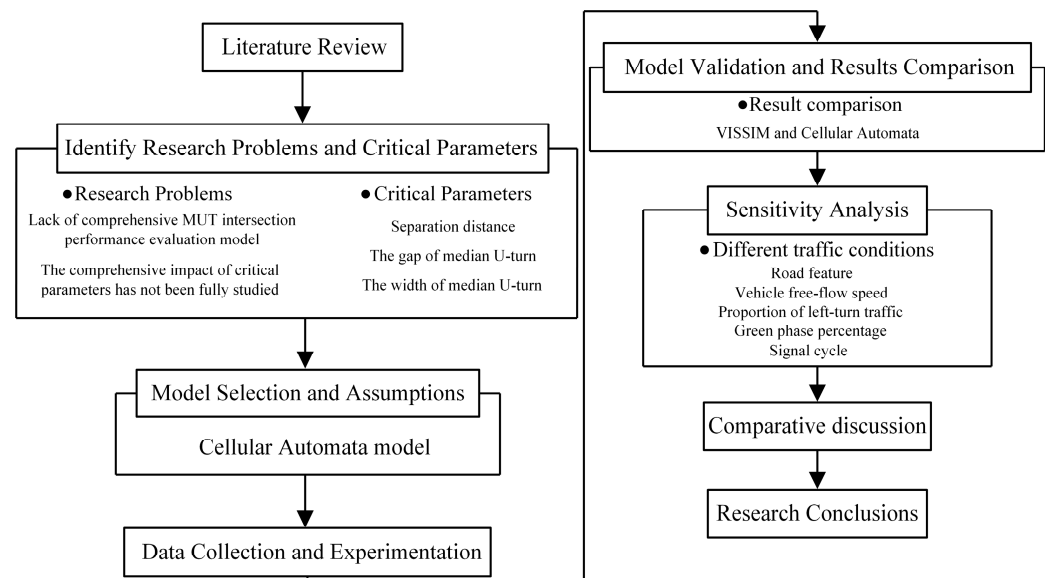


**Figure 3.** The data flow chart for this research.

This article is arranged as follows. Section 2 describes the signal scheme of MUT intersections. In Section 3, the critical parameters of MUT intersections are calculated. The cellular automata model is conducted in Section 4. And Section 5 validates the effectiveness of the cellular automata model. Sensitivity experiments are developed in Section 6. The last section concludes the paper and mentions the future work.

## 2. The Signal Scheme of MUT Intersections

Most MUT intersections have simplified traffic movements by permitting only straight-through movements and indirect left turns. This management approach enables the MUT intersections to utilize a two-phase signal scheme. It assigns the through traffic on major roads and the minor roads into separate signal phases [27,28]. The right-turn traffic on the minor road is not controlled by the signal. The signal phase scheme is illustrated in Figure 4.

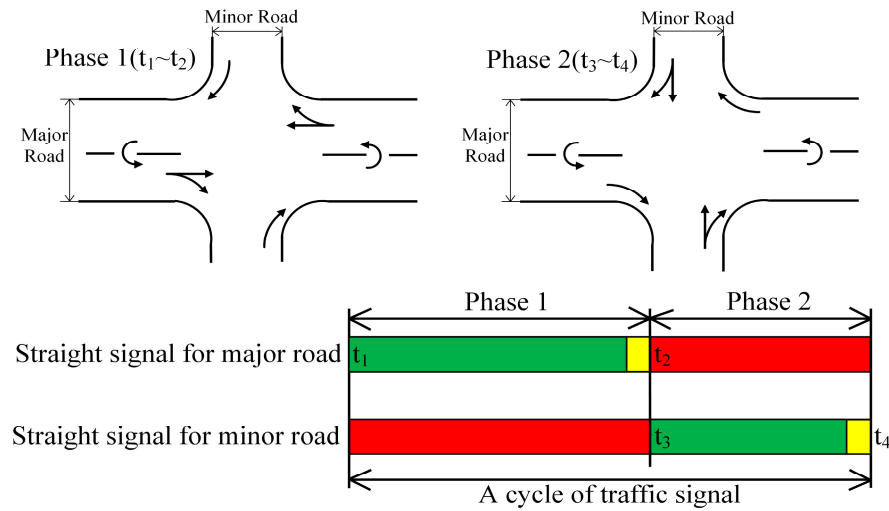


**Figure 4.** Signal timing scheme diagram of MUT intersection.

In phase 1, the through traffic on the major road crosses the intersection, and then travels forward. In contrast, the left-turn traffic on the major road must first proceed straight to reach the median U-turn. Then, it merges with the major road via the median U-turn and finally turns right onto the minor road to complete a left turn. In phase 2, the through traffic on the minor road passes through the intersection. However, the left-turn traffic from the minor road must first turn right to merge with the major road. It then has to change lanes to approach the median U-turn, and subsequently turns around onto the major road. Lastly, it becomes part of the major road traffic and continues straight to complete a left turn.

### 3. Critical Parameter Calculation of MUT Intersections

#### 3.1. The Calculation of the Separation Distance of MUT Intersections

Separation distance refers to the distance between the intersection and the median U-turn. In various unconventional intersection designs, MUT intersections with a correct separation distance usually have greater operational efficiency. Thus, determining the separation distance plays a critical role in the operational performance of MUT intersection. Figure 5 shows the specific segments of the vehicle movement trajectory at an MUT intersection.

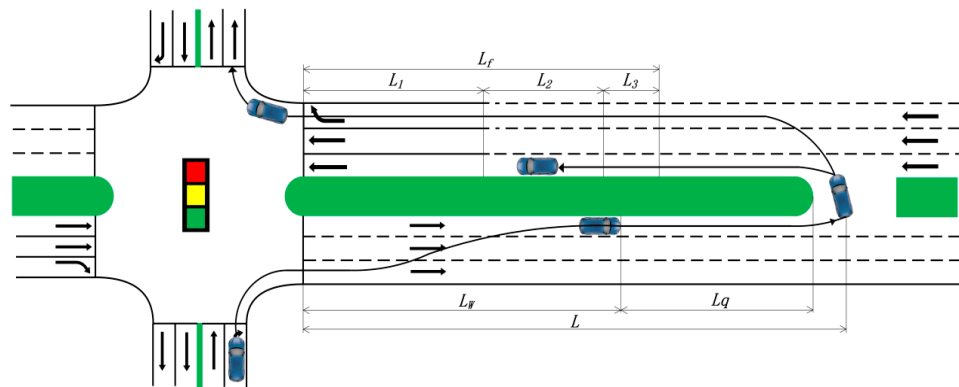


**Figure 5.** The division of different segments in the vehicle movement trajectory in an MUT intersection.

Functional distance is the distance before reaching the stop line at the entrance of an MUT intersection. It represents an important component of the intersection. Entrance lanes within the functional distance often give rise to additional conflicts [29]. Vehicles have to stop in front of the stop line of the MUT intersection during the red phase. The subsequent vehicles need to slow down in order to avoid colliding with the vehicles

queuing ahead. The excessive functional distance may lead to road congestion when traffic is at peak traffic volume. To ensure the operational efficiency of an MUT intersection, the separation distance,  $L$ , must be greater than the functional distance,  $L_f$ . This study divides the functional distance,  $L_f$ , into three sections: the queuing length of vehicles,  $L_1$ ; the deceleration distance of the vehicle,  $L_2$ ; and the vehicle’s perception–reaction distance,  $L_3$ . The functional distance,  $L_f$ , can be calculated as follows:

$$L_f = L_1 + L_2 + L_3 = \frac{\beta_i \times \rho^2}{1 - \rho} N \times l_v + \frac{v^2}{2a} + v \times \tau, \tag{1}$$

$$\rho = \frac{\lambda}{\mu \times N}. \tag{2}$$

where  $\beta_i$  is the proportion of vehicles on each lane to the total number of vehicles at the entrance,  $\rho$  is the service intensity of the intersection,  $N$  is the number of lanes at the entrance of the intersection,  $l_v$  is the average length of the vehicle (m),  $v$  is the speed of the vehicle (m/s),  $a$  is the constant deceleration of the vehicle (m/s<sup>2</sup>),  $\tau$  is the reaction time of the driver within the function area,  $\lambda$  is the average arrival rate of vehicles on the major road (pch/h), and  $\mu$  is the average service rate of the intersection (pch/h).

Because of the unconventional geometric design of the MUT, the traffic on the minor road is bound to first detour onto the major road. It is inevitable that the detoured traffic will combine with the through-straight traffic on the exits of the MUT intersection [30]. The calculation formula for the weaving length,  $L_w$ , based on HCM 2010 is as follows:

$$L_w = \frac{(V_m + V_r) \times w}{S \times (1 - P_w) \times n_w}, \tag{3}$$

where  $V_m$  is the traffic volume of the traffic on the major road entering the intersection exit (pcu/h),  $V_r$  is the traffic volume of the traffic on the minor road entering the intersection exit (pcu/h),  $w$  is the width of a single lane (m),  $P_w$  is the ratio between the weaving traffic volume and total traffic volume at the intersection exit,  $S$  is the lane service level (pcu/h/lane), and  $n_w$  is the number of the lane with weaving traffic.

The turn-around process of the detoured vehicles from the minor road can be considered a queuing model when it enters the major road via a median U-turn. When the gap between each vehicle in the traffic on the major road is large enough for one vehicle to enter the it, a queuing vehicle can merge directly onto the major road. Otherwise, the queuing vehicles will have to wait outside the median U-turn. The arrival of the detoured vehicles at the median U-turn can be regarded to follow the Poisson distribution. The gap between each vehicle in the traffic on the major road can be regarded as following the Erlang distribution. Thus, the turn-around process of the detoured traffic can be considered as following the  $M/E_K/1$  queuing model.

Assuming the number of vehicles turning around via the median U-turn is  $n$  ( $n \geq 1$ ),  $t_i$  is the time at which the  $i$ th vehicle completely merges onto the major road, and  $t$  is the time headway of the traffic flow on the major road. When the time headway of major traffic meets the requirement for  $n$  vehicles to turn around, then  $n$  vehicles can turn around [31]. Therefore, we can conclude that:

$$t_i \leq t \leq \sum_i^{i+1} t_i, \tag{4}$$

$$p_n = \int_{t_i}^{\sum_i^{i+1} t_i} p(t) dt = \int_{t_i}^{\sum_i^{i+1} t_i} \frac{\lambda k (\lambda k t)^{k-1}}{(k-1)!} e^{-\lambda k t} dt, \tag{5}$$

$$u = \sum_{n=1}^{\infty} (1 - \lambda) p_n, \tag{6}$$

where  $p_n$  is the probability of the detoured traffic that merges with the major road,  $k$  is the order of the Erlang distribution, and  $u$  is the service rate of the median U-turn.

According to the  $M/E_k/1$  queuing model, the queuing length of vehicles outside the median U-turn,  $L_q$ , can be calculated:

$$L_q = \frac{(k+1)\left(\frac{\lambda}{u}\right)^2}{2k\left(1 - \frac{\lambda}{u}\right)}. \quad (7)$$

Considering traffic safety, it should ensure that the separation distance,  $L$ , is slightly greater than the sum of the weaving length,  $L_w$ , and the queuing length of vehicles outside the median U-turn,  $L_q$ , because this can provide sufficient space for vehicles to complete the necessary weaving and queuing maneuvers and prevent congestion. Above all, the separation distance,  $L$ , can be determined as follows:

$$L \geq \max\{L_f, (L_w + L_q)\}. \quad (8)$$

### 3.2. The Calculation of the Gap of the Median U-Turn of MUT Intersections

The gap of the median U-turn is a critical factor affecting the operation of turn-around vehicles. An effective gap between different fast-moving vehicles should be provided in the approaching through traffic [32,33]. The gap of the median U-turn must ensure that there is no collision between the turn-around vehicles and straight-through vehicles. To avoid potential rear-end accidents, motorists must be able to observe the approaching vehicles within a limited sight distance and react quickly to control the vehicle properly. The area needed to provide this unobstructed view is called the Clear Sight Triangle [34,35]. Figure 5 shows the movements of vehicles through the median U-turn. Based on the description above, this paper combines the Clear Sight Triangle with the vehicle operation process to determine the maximum gap for median U-turns. Thus, the following assumptions can be made:

1. The traffic volume at the intersection remains stable.
2. Turn-around vehicles and straight-through vehicles all have a clear view of each other.
3. Drivers only turn around when there is a sufficient gap, and the speed of the turn-around remains constant during the turning around of the vehicles.
4. Each vehicle in the same group of turn-around vehicles takes the same time to pass through the median U-turn.

The operation process of vehicles on the minor road crossing the median U-turn is shown in Figure 6. The vehicle on the minor road (*Car P*) first departs from position  $P_1$  to turn right to enter the major road. It will weave with the vehicles on the major road. Then, *Car P* arrives at position  $P_2$  with the average weaving speed  $v_i$  (m/s) to wait to turn around. When *Car P* is at position  $P_2$ , the oncoming vehicle on the major road (*Car C*) is at position  $C_1$ . *Car C* starts decelerating from speed  $v_c$  ( $v_c > v_i$ ) (m/s) with a constant acceleration of  $a_c$  ( $m/s^2$ ). *Car P* departs from position  $P_2$  to cross the median U-turn via position  $P_3$ . It can be considered that *Car P* has completed the turn around when its rear end is appropriately at  $A_2$  point. *Car C* has decelerated to speed  $v_i$  at this moment; its headstock is appropriately at  $A_1$  point. In this paper, we consider the variable  $G$  to be the critical gap between *Car P* and *Car C* at this moment. The critical gap is a vital factor for vehicle safety operation. It is essentially the drivers' acceptance of the minimum distance between two adjacent vehicles [36]. The critical gap will be beneficial for determining the maximum gap of the median U-turn to determine its safety effectiveness. After ensuring that there is no collision between *Car P* and *Car C*, *Car P* begins to accelerate in order to quickly pass through the intersection. Then, *Car C* will maintain a uniform speed of  $v_i$  until *Car P* and *Car C* reach the safe following distance,  $L_R$  (m). Subsequently, *Car C* starts accelerating to follow *Car P*. The movement processes of *Car P* and *Car C* are as follows:

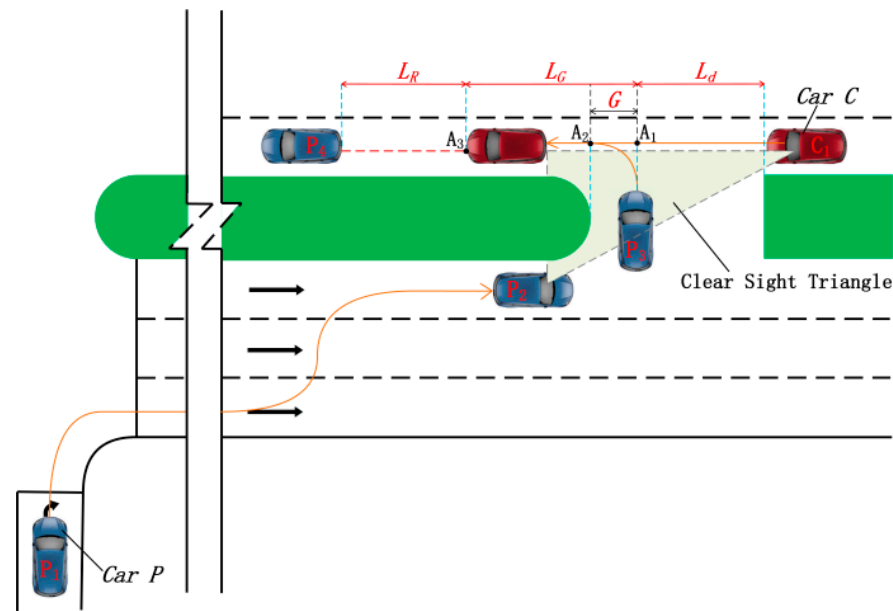


**Figure 6.** The vehicles' operation processes in the median U-turn.

I. The deceleration process of Car C.

Assuming the time it takes for Car P to complete the turn around from position P<sub>2</sub> is  $\varphi$  (s), the reaction time of the driver approaching the median U-turn is  $\gamma$  ( $\varphi > \gamma$ ) (s). The deceleration distance of Car C  $L_d$  can be calculated as follows:

$$L_d = (2\varphi - \gamma) \times v_c - \frac{1}{2}(\varphi - \gamma)^2 \times a_c, \tag{9}$$

II. The uniform speed driving process of Car C.

Assuming that the distance that Car C travels by Car C at a uniform speed,  $L_G$ , the time for Car C to pass the critical gap,  $G$ , is  $t_G$  (s). We can obtain:

$$L_G = v_i \times t_j = G + |A_2A_3| = v_i \times t_G + |A_2A_3|, \tag{10}$$

III. The acceleration process of Car P.

Assuming that Car P accelerates from speed  $v_i$  to speed  $v_L$  (m/s) with a constant acceleration,  $a_L$  (m/s<sup>2</sup>), until the distance between Car P and Car C reaches the safe following distance,  $L_R$ . The time taken for Car P to accelerate is  $t_j$  (s). Thus, we can obtain:

$$v_L^2 - v_i^2 = 2a_L \times (L_R + |A_2A_3|), \tag{11}$$

$$v_L = v_i + a_L t_j, \tag{12}$$

By combining the equations above, we can obtain:

$$t_G = \frac{L_R}{v_i} - \frac{(v_L - v_i)^2}{2a_L v_i}. \tag{13}$$

Because of the unconventional geometric design of the MUT, the traffic on the minor road must first detour onto the major road. Unlike the traffic on the major road, the traffic from the minor road has to change lanes twice or more to approach the median U-turn [37]. Thus, the detoured traffic is likely to form a weaving segment with the through traffic. The average speed of weaving traffic has to be estimated [38]. The average speed of vehicles within the weaving segment,  $v_i$ , can be obtained:

$$v_i = v_{\min} + \frac{v_{\max} - v_{\min}}{1 + W_i}, \tag{14}$$

$$W_i = \frac{a(1 + V_R)^b \left(\frac{q}{n}\right)^c}{(3.28L_w)^d}, \tag{15}$$

where  $W_i$  is the intensity of the weaving traffic or non-weaving traffic,  $V_R$  is the weaving traffic ratio,  $q_i$  is the total traffic volume within the weaving zone (pcu/h),  $n$  is the number of lanes within the weaving zone,  $a, b, c, d$  is the constant,  $v_{max}$  is the maximum possible speed within the weaving zone (m/s),  $v_{min}$  is the minimum possible speed within the weaving zone (m/s), and  $L_w$  is the length of the weaving section (m). Table 1 records the distribution of constants for Equation (15).

**Table 1.** Distribution of constants under different weaving conditions.

Constraint Type	With the Weaving Traffic Within the Weaving Zone				Without the Weaving Traffic Within the Weaving Zone			
	a	b	c	d	a	b	c	d
Non-constrained	0.08	2.3	0.8	0.6	0.002	6.0	1.1	0.6
Constrained	0.14	2.3	0.8	0.6	0.002	6.0	1.1	0.6

For all drivers, it is important to keep a certain safe following distance from the vehicle in front when driving. A safe following distance gives drivers time to see, think, and act. Under normal road conditions, the safe following distance should be a minimum of three seconds (three-second rule) [39–41]. It is worth noting that there is still no standardized guideline to calculate the safe following distance. The three-second rule is still widely adopted by transportation departments around the world. The safe following distance calculated based on the different vehicle driving speeds at urban intersections is summarized in Table 2.

**Table 2.** Safe following distance of vehicles under different vehicle driving speeds at urban intersections.

Normal Conditions	Speed(km/h)					
	10	20	30	40	50	60
Safe Following Distance (m)	8.5	17	25	33	42	51

So, the maximum gap of the median U-turn,  $L_{max}$ , can be concluded:

$$L_{max} = G + L_d. \tag{16}$$

Figure 7 shows the minimum gap for vehicles turning around at a median U-turn. The minimum gap for vehicles at the median U-turn denoted as  $L_{min}$  is defined as: the difference between the outermost trajectory radius,  $R_o$ , and the innermost trajectory radius,  $R_t$ , of the turning vehicle when it turns around with the minimum radius of the vehicle turn around, and adding the double values of the edge security distance,  $G_s$ . Figure 6 shows the trajectory of vehicles turning around.

So, we can determine the calculation formula for the minimum gap of the median U-turn,  $L_{min}$ :

$$L_{min} > R_o - R_t + 2G_s, \tag{17}$$

$$R_o = R_w + W_h = \frac{d_w}{\sin \theta_w} + W_h, \tag{18}$$

$$R_t = R_i - W_h = \frac{d_w}{\tan \theta_n} - W_h, \tag{19}$$

where  $R_w$  is the radius of turning around for outer wheels (m),  $R_i$  is the radius of turning around for inner wheels (m),  $W_h$  is the width of half a vehicle wheel (m),  $d_w$  is the wheelbase of the vehicle for turning around (m),  $\theta_w$  is the outer wheel angle of the vehicle (deg), and  $\theta_n$  is the inner wheel angle of the vehicle (deg).

Based on the points above, the range of values for the gap of the median U-turn,  $L_{gap}$ , can be obtained:

$$L_{min} < L_{gap} \leq L_{max}. \tag{20}$$

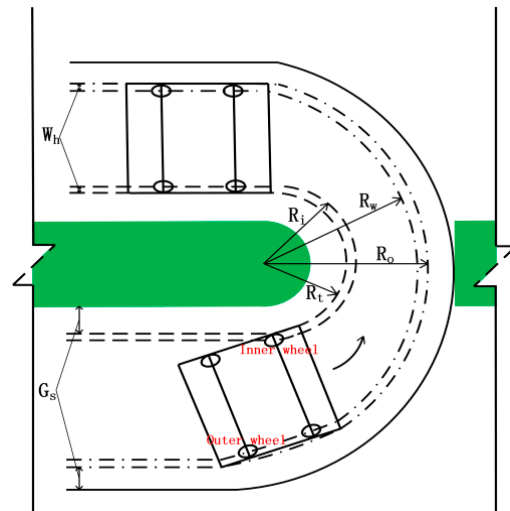


Figure 7. The minimum gap of the median U-turn.

### 3.3. The Calculation for the Width of the Median U-Turns at MUT Intersections

The trajectory of vehicles within median U-turns can be approximated as a semicircular arc. Wael et al. combine the circular curvature and the trajectory of vehicle turns to develop the Euler spiral curve for vehicle turning paths. The Euler spiral curve is the transition between a straight line and circular curve [42,43]. It prevents drivers from turning suddenly when entering a median U-turn. This curve can be applied to the trajectory of vehicles turning around at the median U-turn. The formula for the Euler spiral curve can be described as:

$$R_s L_s = A^2, \tag{21}$$

where  $R_s$  is the radius of the Euler spiral curve,  $L_s$  is the distance between the vehicle and the beginning (or ending) of the Euler spiral curve, and  $A$  is the parameter of the Euler spiral curve.

Figure 8 shows that the trajectory of the detoured vehicle is approximately a semicircle when the vehicle turns around. This trajectory is divided into three segments: the entering Euler spiral curve segment (orange line), the circular curve segment (blue line), and the exit Euler spiral curve segment (red line). The center of the entering and exit Euler spiral curve segments is at the intersection point of the perpendicular bisectors of the beginning and ending tangents.

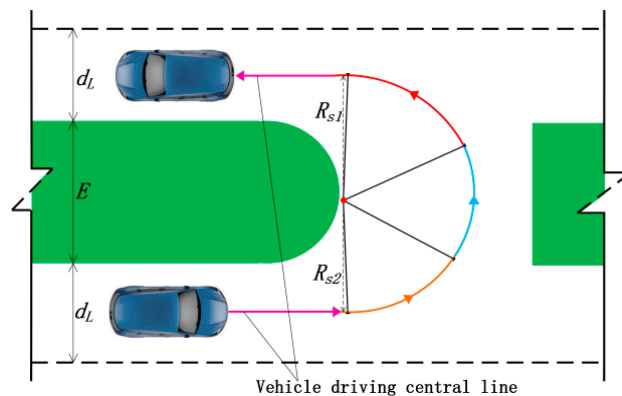


Figure 8. The width of the median U-turn.

The width of the median U-turn can be calculated as follows:

$$E \geq R_{s1} + R_{s1} - d_L \tag{22}$$

where  $R_{s1}$  is the radius of the exit Euler spiral curve segment.  $R_{s2}$  is the radius of the entering Euler spiral curve segment.  $d_L$  is the width of a single lane.

#### 4. The Cellular Automata of MUT Intersections

As a specific methodology for describing the macroscopic characteristics of traffic flow, cellular automata have been widely applied to reproduce complex traffic situations in a discrete space [44,45]. In this section, a cellular automata model of a specific MUT intersection is proposed. It describes the operation rules of vehicles within the MUT intersection on the basis of real traffic phenomena. The calculation theory of vehicle delay is also mentioned at the end of this section. The cellular automata model of the MUT intersection is shown in Figure 9.

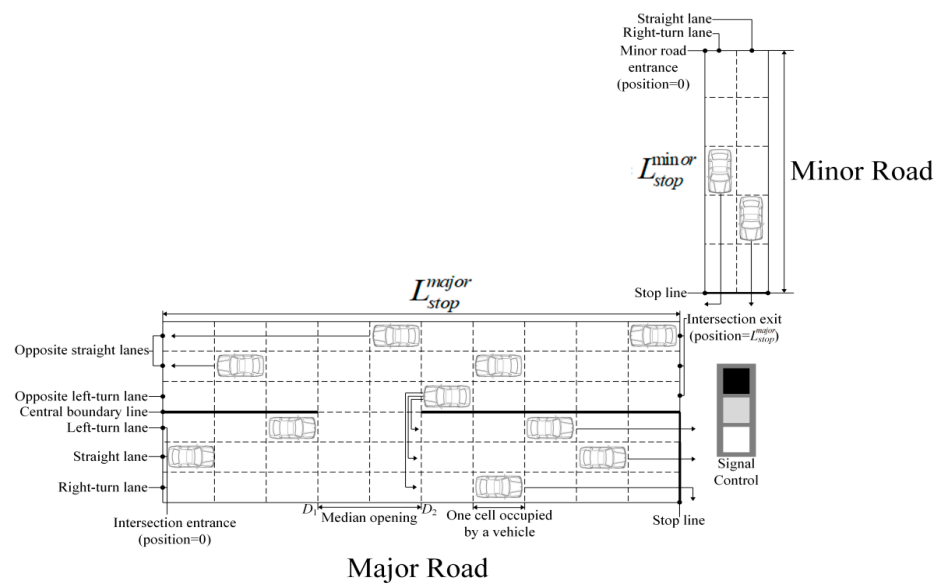


**Figure 9.** The traffic scene at MUT intersections simulated by the cellular automata model.

To facilitate the calculation of vehicle delay, certain conditions or parameters that may affect the operation of the MUT intersection need to be simplified. Details are as follows.

1. Any lane at the MUT intersection will not be in an over-saturated state to ensure the queuing vehicles are able to dissipate completely during the green phase.
2. Any lane at the MUT intersection will not prevent vehicles from change lanes.
3. The impact of vehicle types on vehicle movements is not considered.
4. The average vehicle arrival rate and saturation flow rate remain unchanged during the selected time.
5. The effect of the width of the median U-turn on vehicle operation is not considered.

##### 4.1. Establishment of the Vehicle Initial State

The speed of each vehicle, the position of each vehicle, and the direction in which each vehicle is moving (left turn, straight, or right turn) are all critical elements in the cellular automata. These parameters need to be defined rationally. In addition, in order to replicate a realistic scenario, it is necessary to simultaneously take into account both the major road and minor road when defining dynamic vehicle inputs.

First, the initial speed for each vehicle is randomly determined within a selected range. The initial position of any vehicle is assigned randomly at the first cells at the entrances of different lanes. The generation probability for vehicles at the entrances of the major road

and minor road is based on the flow proportion of traffic in different directions in a mixed traffic flow. Then vehicles moving in different directions will be randomly generated using this probability.

The initial state of the vehicles at the intersection entrance is as follows:

$$\begin{cases} Car_{major\_v_i}(0) = 1 + \text{fix} \left[ \text{rand}() \times (v_{\max}^{major} - 1) \right] \\ Car_{major\_lane_i}(0) = \text{fix} \left[ \text{rand}() \times N_{entrance}^{major} \right] \\ Car_{major\_position_i}(0) = 1 \end{cases}, \quad (23)$$

The initial state of the vehicles on the minor road is as follows:

$$\begin{cases} Car_{minor\_v_i}(0) = 1 + \text{fix} \left[ \text{rand}() \times (v_{\max}^{minor} - 1) \right] \\ Car_{minor\_lane_i}(0) = 1 + \text{fix} \left[ \text{rand}() \times N_{road}^{minor} \right] \\ Car_{minor\_position_i}(0) = 1 \end{cases}, \quad (24)$$

Because of the specific operation mode of MUT intersections, the left-turn and right-turn traffic on the minor road will converge into the same mixed flow and simultaneously enter the opposite lanes. So, the generation probability of the vehicles at the intersection exit has to also consider the proportion of the left-turn traffic on the minor road in the minor traffic flow. This probability will be an important basis for the generation of vehicles on the opposite road. The initial state of the vehicles at the intersection exit is follows:

$$\begin{cases} Car_{opposite\_v_i}(0) = 1 + \text{fix} \left[ \text{rand}() \times (v_{\max}^{major} - 1) \right] \\ Car_{opposite\_lane_i}(0) = \text{fix} \left[ \text{rand}() \times (N_{entrance}^{opposite} - 1) \right] \\ Car_{opposite\_position_i}(0) = L_{stop}^{major} - 1 \end{cases}, \quad (25)$$

where  $Car_{major\_v_i}(0)$  indicates the initial speed of the  $i$ th vehicle at the intersection entrance.  $Car_{major\_lane_i}(0)$  indicates which type of lane the  $i$ th vehicle at the intersection entrance is on.  $Car_{major\_position_i}(0)$  indicates the initial position of the  $i$ th vehicle at the intersection entrance.  $Car_{minor\_v_i}(0)$  indicates the initial speed of the  $i$ th vehicle at the minor road entrance.  $Car_{minor\_lane_i}(0)$  indicates which type of lane the  $i$ th vehicle at the minor road entrance is on.  $Car_{minor\_position_i}(0)$  indicates the initial position of the  $i$ th vehicle at the minor road entrance.  $Car_{opposite\_v_i}(0)$  indicates the initial speed of the  $i$ th vehicle at the intersection exit.  $Car_{opposite\_lane_i}(0)$  indicates which type of lane the  $i$ th vehicle at the intersection exit is on.  $Car_{opposite\_position_i}(0)$  indicates the initial position of the  $i$ th vehicle at the intersection exit.  $v_{major\ max}$  indicates the maximum speed limitation of the major road.  $v_{minor\ max}$  indicates the minimum speed limitation of the minor road.  $N_{major\ entrance}$  indicates the number of lanes at the major road entrance.  $N_{minor\ road}$  indicates the number of lanes at the minor road entrance.  $N_{opposite\ entrance}$  indicates the number of lanes at the intersection exit.

The travel model equation of vehicles at the intersection entrance is as follows:

$$\text{Direction} = \begin{cases} 0, & \text{if } \text{rand}() \leq p_i^{entrance} \\ 1, & \text{if } p_i^{entrance} < \text{rand}() \leq p_i^{entrance} + p_s^{entrance} \\ 2, & \text{otherwise} \end{cases}, \quad (26)$$

The travel model formula of vehicles at the intersection exit is as follows:

$$\text{Direction} = \begin{cases} 0, & \text{if } p_i^{exit} \times p_r^{minor} < \text{rand}() \leq p_i^{exit} \\ 1, & \text{if } p_s^{exit} \times p_r^{minor} < \text{rand}() \leq p_s^{exit} \end{cases}, \quad (27)$$

The travel model formula of vehicles at the minor road entrance is as follows:

$$\text{Direction} = \begin{cases} 1, & \text{if } \text{rand}() \leq p_s^{minor} \\ 2, & \text{otherwise} \end{cases}, \quad (28)$$

where  $P_{entrance\ l}$  indicates the proportion of left-turn traffic in a mixed traffic flow that enters the intersection entrance.  $P_{entrance\ s}$  indicates the proportion of through traffic of mixed traffic flow that enters the intersection entrance.  $P_{exit\ l}$  indicates the proportion of left-turn traffic of a mixed traffic flow that enters the intersection exit.  $P_{exit\ s}$  indicates the proportion of through traffic of a mixed traffic flow that enters the intersection exit.  $P_{minor\ l}$  indicates the proportion of left-turn traffic of a mixed traffic flow that enters the minor road entrance.  $P_{minor\ s}$  indicates the proportion of through traffic of a mixed traffic flow that enters the minor road entrance.  $P_{minor\ r}$  indicates the proportion of right-turn traffic of a mixed traffic flow that enters the minor road entrance. And the sum of  $P_{major\ l}$  and  $P_{major\ s}$  is less than 1. The sum of  $P_{exit\ l}$  and  $P_{exit\ s}$  is less than 1. The sum of  $P_{minor\ l}$ ,  $P_{minor\ s}$ , and  $P_{minor\ r}$  equals to 1.

Different numbers represent the type of vehicle movement direction. The type of number is determined as follows:

$$\text{Type} = \begin{cases} 0, & \text{Turn left} \\ 1, & \text{Straight – through} \\ 2, & \text{Turn right} \end{cases} \quad (29)$$

The total number of vehicles on the major road and minor road becomes the critical reference for determining whether new vehicles can be generated after setting the initial status.

#### 4.2. Rules for Vehicle Operation

##### 4.2.1. Speed Enhancement Rule

Each vehicle will update its speed based on the current speed and acceleration. The speed update equation is as follows:

$$v_i(t + 1) = \min[v_i(t) + a_i(t) \times \Delta t, v_{max}], \quad (30)$$

where  $v_i(t)$  is the speed of the  $i$ th vehicle at time  $t$ .  $a_i(t)$  is the acceleration of the  $i$ th vehicle at time  $t$ .  $\Delta t$  is the unit time.  $v_{max}$  is the maximum speed of the vehicle ( $v_{max} \leq v_{major\ max}$  and  $v_{max} \leq v_{minor\ max}$ ).

##### 4.2.2. Speed Reduction Rule

This paper proposes a speed reduction rule to prevent vehicles from colliding with the vehicle in front. The speed reduction equation is as follows:

$$v_i(t + 1) = \min[v_i(t), d_{front}(i) - D_{safe}], \quad (31)$$

where  $d_{front}(i)$  is the distance between the  $i$ th vehicle and the front vehicle.  $D_{safe}$  is the driving security distance.

##### 4.2.3. Random Slowing Rule

Vehicle speed reduction may occur when driving because of many various uncertain factors. Thus, this paper introduces a random slowing rule for vehicles.

$$v_i(t + 1) = \max[v_i(t) - 1, 0] \text{ if } \text{rand}() < p_{slow}, \quad (32)$$

where  $p_{slow}$  is the probability of the vehicle random slowing value.

##### 4.2.4. Location Update

Each vehicle will update its location based on the current speed. The location update equation is as follows:

$$x_i(t + 1) = x_i(t) + v_i(t + 1) \times \Delta t. \quad (33)$$

where  $x_i(t)$  is the location of the  $i$ th vehicle at time  $t$ .

### 4.3. Rules for a Vehicle Changing Lanes

In the free-driving process, vehicles are supposed to change to the corresponding lane to maintain the correct direction of travel. The behavior of a vehicle changing lanes will inevitably induce changes in the vehicle’s speed and acceleration. Moreover, drivers have to consider the security distance between the front vehicle and rear vehicle before the current vehicle changes lanes. Therefore, it is important to establish reasonable lane-changing rules to study the operation of traffic flow.

To ensure the safety of vehicle lane-changing, vehicles that need to change lanes should maintain a sufficient safety distance in front and behind. The vehicle lane-changing rule is as follows:

$$\begin{cases} \text{type}_i \neq \text{lane}_i \\ D_{\text{front,new}} \geq [v_i(t) + a_i(t) \times \Delta t] \times \Delta t + D_{\text{safe}} \\ D_{\text{back,new}} \geq [v_{i-1}^{\text{back}}(t) + a_{i-1}^{\text{back}}(t) \times \Delta t] \times \Delta t + D_{\text{safe}} \\ p_w > \text{rand}() \end{cases} \quad (34)$$

where  $D_{\text{front,new}}$  is the distance between the vehicle that needs to change lanes on the current lane and the vehicle ahead on the target lane.  $D_{\text{back,new}}$  is the distance between the vehicle that needs to change lanes on the current lane and the rear vehicle on the target lane.  $v_{\text{back}}(t)$  is the speed of the vehicle behind the current vehicle.  $a_{\text{back}}(t)$  is the acceleration of the vehicle behind the current vehicle.  $p_w$  is the probability of the current vehicle changing lanes. It reflects the willingness of a driver to change lanes.

### 4.4. Rules for Vehicle Movements Under Signal Control

Before entering the intersection, the movements of each vehicle in every direction depend on the status of the traffic signal.  $t_{\text{major } s}$  is the time of the straight signal in the major road signal phase.  $t_{\text{minor } s}$  is the time of the straight signal in the minor road signal phase.  $t_1, t_2, t_3, t_4$  are shown in Figure 3.  $t_{\text{major } s} = 0$  ( $t_{\text{minor } s} = 0$ ) represents the beginning of the signal period.  $t_{\text{major } s}$  ( $t_{\text{minor } s}$ ) increases by one unit with each time step. If  $t_{\text{major } s}$  ( $t_{\text{minor } s}$ ) equals the cycle of the traffic signal,  $t_c$ , then  $t_{\text{major } s}$  ( $t_{\text{minor } s}$ ) will change back to 0, and a new traffic signal cycle begins. The specific motion rules for vehicles passing through the intersection are as follows.

Normally, right-turn traffic is not controlled by the traffic signal at an unchannelized intersection. Consequently, vehicles on the major road are only permitted to turn right while passing the intersection when the traffic signal is red. Other vehicles have to stay behind the stop line on the major road. The formula for vehicle movements on the major road, based on signal control, can be concluded as follows:

$$x_i(t+1) = \begin{cases} x_i(t), & \text{if } \begin{cases} t_s^{\text{major}} \notin (t_1, t_2) \\ x_i(t) = L_{\text{stop}}^{\text{major}} - 1 \\ \text{Direction} \neq 2 \end{cases} \\ x_i(t) + v_i(t+1), & \text{otherwise} \end{cases} \quad (35)$$

Similar to the right-turn traffic on the major road, the formula for vehicle movements on the minor road, based on signal control, can be concluded as follows:

$$x_i(t+1) = \begin{cases} x_i(t), & \text{if } \begin{cases} t_s^{\text{minor}} \notin (t_3, t_4) \\ x_i(t) = L_{\text{stop}}^{\text{minor}} - 1 \\ \text{Direction} = 1 \end{cases} \\ x_i(t) + v_i(t+1), & \text{otherwise} \end{cases} \quad (36)$$

where  $L_{\text{major stop}}$  ( $L_{\text{minor stop}}$ ) is the distance between the entrance of the major road (minor road) to the stop line of the major road (minor road).

#### 4.5. Rules for Vehicle Movements at the Median U-Turn

After turning around via the median U-turn, the left-turn traffic on the major road will become the right-turn traffic of the major road and leave the intersection to complete a left turn. The equation for the left-turn traffic on the major road through the median U-turn is as follows:

$$x_i(t+1) = \begin{cases} x_i(t) - v_i(t), & \text{if } \begin{cases} x_i(t) \in (D_1, D_2) \\ \text{Direction} = 0 \\ \text{Car}_{\text{opposite\_lane}_i}(0) = 0 \end{cases} \\ x_i(t) + v_i(t+1), & \text{otherwise} \end{cases} \quad (37)$$

The equation for the left-turn traffic on the major road after turning around via the median U-turn is as follows:

$$\begin{cases} \text{Car}_{\text{major\_lane}_i}(t) = \text{fix}[\text{rand}() \times N_{\text{road}}^{\text{major}}] \\ \text{Car}_{\text{major\_position}_i}(t) > D_1 \\ \text{Direction} = 2 \\ v_i(t+1) = -v_i(t) \\ x_i(t+1) = x_i(t) - v_i(t) \end{cases} \quad (38)$$

After turning around via the median U-turn, the left-turn traffic on the minor road will become the through traffic of the major road and drive forward to complete a left turn. The equation for the left-turn traffic on the minor road through the median U-turn is as follows:

$$x_i(t+1) = \begin{cases} x_i(t) - v_i(t), & \text{if } \begin{cases} x_i(t) \in (D_1, D_2) \\ \text{rand}() < p_1^{\text{minor}} \\ \text{Car}_{\text{opposite\_lane}_i}(0) = 0 \end{cases} \\ x_i(t) + v_i(t+1), & \text{otherwise} \end{cases} \quad (39)$$

The equation for the left-turn traffic on the minor road after turning around via the median U-turn is as follows:

$$\begin{cases} \text{Car}_{\text{major\_lane}_i}(t) = \text{fix}[\text{rand}() \times (N_{\text{road}}^{\text{major}} - 1)] \\ \text{Car}_{\text{major\_position}_i}(t) > D_1 \\ \text{Direction} = 1 \\ v_i(t+1) = -v_i(t) \\ x_i(t+1) = x_i(t) - v_i(t) \end{cases} \quad (40)$$

#### 4.6. Vehicle Delay Calculation

This paper uses cellular automata to calculate the total delay at the MUT intersection. The equation for vehicle delays on the major road can be concluded as:

$$\text{Delay}_{\text{major}} = \sum_{\text{type}=0}^2 \left( \sum_{t=1}^T N_{\text{major}}^{\text{type}} \times \Delta t - \frac{L_{\text{stop}}^{\text{major}}}{V_{\text{max}}^{\text{major}}} \times N_n^{\text{type}} \right) \quad (41)$$

The equation for vehicle delays on the minor road can be concluded as:

$$\text{Delay}_{\text{minor}} = \sum_{\text{type}=0}^2 \left( \sum_{t=1}^T N_{\text{minor}}^{\text{type}} \times \Delta t - \frac{L_{\text{stop}}^{\text{minor}}}{V_{\text{max}}^{\text{minor}}} \times N_n^{\text{type}} \right) \quad (42)$$

Therefore, the total vehicle delay,  $D_{\text{total}}$ , is as follows:

$$D_{\text{total}} = \text{Delay}_{\text{major}} + \text{Delay}_{\text{minor}} \quad (43)$$

The average vehicle delay,  $D_{aver}$ , is:

$$D_{aver} = \frac{D_{total}}{N_s}. \tag{44}$$

where  $Delay_{major}$  indicates the total delay of each vehicle’s direction traveling on the major road.  $Delay_{minor}$  indicates the total delay of each vehicle’s direction traveling on the minor road.  $N_{major\ type}$  indicates the total number of vehicles that appear in each type of lane at the intersection entrance and intersection exit per unit of time.  $N_{minor\ type}$  indicates the total number of vehicles that appear in each type of lane at minor road entrances per unit of time.  $\Delta t$  indicates the unit simulation time.  $N_{type\ n}$  indicates the total number of vehicles that travel in the lane of a corresponding type.  $N_s$  is the total number of vehicles simulated in the cellular automata.

### 5. Model Effectiveness Validation

In this section, we carry out simulation validation by applying field data to investigate the accuracy of the cellular automata model. Average vehicle delay will be the evaluation criterion to compare the difference between the cellular automata model and traffic simulation model under various traffic volumes. Average vehicle delay is a primary indicator for evaluating the operational performance of signalized intersections [46]. All the results will help determine whether the cellular automata model is suitable for assessing the complex traffic conditions at MUT intersections.

#### 5.1. Field Data Collection

To verify the effectiveness of the proposed cellular automata model, the field traffic volume data of a specific MUT intersection located in Xi’an are used to input into the model. Figure 10 illustrates the real scene of a certain MUT intersection on Chang’an Street, Xi’an city, China. This MUT intersection consists of a two-way, four-lane (minor road) road from north to south and a two-way, six-lane (major road) road from west to east. There are three intersection entrance lanes with a left-turn lane, straight lane, and right-turn lane on the major road. And the minor road only has two intersection entrance lanes with a straight lane and right-turn lane. A median U-turn is set up on the west and east sides of this intersection. The distances from the selected MUT intersection to the other two adjacent intersections are approximately 460 m and 610 m. The current parameters measured for the selected MUT intersection are shown in Table 3.



Figure 10. The scene of the selected MUT intersection in Xi’an city (adapted from Google Earth).

Table 3. The current parameters of the selected MUT intersection.

Current Parameters	Separation Distance (m)	Gap of Median U-Turn (m)	Width of Median U-Turn (m)
Sides of intersection	East	116	4
	West	80	

In this paper, we investigate vehicle data at different entrances of the MUT intersection on Chang'an Street. Video cameras were installed at each entrance to obtain the traffic field data over five consecutive working days. With a larger traffic flow, traffic congestion during this period is more serious in the morning peak hours. The traffic volume at the MUT intersection during peak hours is presented in Table 4.

**Table 4.** Traffic data at the entrance of the selected MUT intersection during peak hours.

Direction		Day 1	Day 2	Day 3	Day 4	Day 5
		Traffic Flow (veh/h)				
East entrance	Left turn	176	167	157	169	164
	Straight through	733	766	735	746	772
	Right turn	147	123	139	143	151
West entrance	Left turn	182	190	187	174	193
	Straight through	774	765	721	760	780
	Right turn	158	163	142	161	160
South entrance	Left turn	105	119	106	103	112
	Straight through	159	147	135	137	149
	Right turn	32	46	41	39	47
North entrance	Left turn	96	85	83	91	90
	Straight through	162	152	138	166	157
	Right turn	43	55	39	47	51
Total (veh/h)		2767	2778	2623	2736	2826

This MUT intersection employs two-phase signal control. The through movements of vehicles on the major road and minor road are assigned phases. Left turns for vehicles are prohibited within the intersection. The right-turn movements of vehicles are not controlled by traffic signals. The signal cycle of this MUT intersection is 100 s. The green duration for the through movements on the major road is 52 s. The red duration for the through movements on the minor road is 42 s. The yellow duration is 3 s.

### 5.2. Simulation Construction

To examine the reliability of the proposed cellular automata model, we will employ commercial simulation software VISSIM (Version 4.0) to construct a traffic simulation model based on a realistic traffic scenario. As a leading simulation software, VISSIM can present a vehicle operation environment under different conditions, such as lane type, traffic composition, and traffic signal control [47,48]. Because of the similar operating rules, the VISSIM model can serve as a comparison for the proposed cellular automata model. Subsequently, we compare the average vehicle delay simulated by the two models to demonstrate the consistency between the cellular automaton model and the microsimulation model in different scenarios. Therefore, the VISSIM model based on the current situation of the selected MUT intersection is built first. Then, based on the calculation results in Chapter 3, the modified VISSIM model for the selected MUT intersection is also constructed. The modified parameters of the MUT intersection are presented in Table 5.

The VISSIM model for the current MUT intersection is built using the parameters obtained from the field. According to Table 5, the VISSIM model for the modified MUT intersection is also developed. It should be noted that the east and west sides of the modified MUT intersection model each require an exclusive separation distance. According to Equation (8), the appropriate separation distance,  $L$ , for the selected intersection is slightly greater than the calculated value. Therefore, the separation distance on the west side of the intersection is 92 m, and the separation distance on the east side of the intersection is 124 m.

Similarly, the gap and width of the median U-turn should be considered to use an identical method. Therefore, based on Table 5, the gap and width of the median U-turn

are 8 m and 10 m, respectively. Additionally, the signal cycle of both VISSIM models is consistent with that of the selected intersection. All the parameters required for building the simulation models have been obtained.

**Table 5.** The modified parameters for the selected MUT intersection.

Modified Parameters	Direction	Periods				
		Day 1	Day 2	Day 3	Day 4	Day 5
Separation distance (m)	East	119.5	121	117.2	119.2	123.3
	West	88.8	90.3	85.4	88.1	91.6
Gap of median U-turn (m)	East	$5.7 < L_{gap} \leq 10.5$				
	West					
Width of median U-turn (m)	East	$E \geq 7.6$				
	West					

In this paper, the cellular automata models are simulated using MATLAB. We will provide two versions of the cellular automata model separately: one with the current parameters and the other with modified parameters. The total lengths of the major road on the east and west sides of the selected intersection are 150 cells and 100 cells, respectively. The total length of the minor road on the north and south sides of the selected intersection is 120 cells. One vehicle occupies one cell, and the length of each cell is 4 m. No central boundary line is placed at specific locations of certain cells on the major road to simulate median U-turn operations. The new vehicles in the two cellular automata models are generated as described in Section 4. Considering the speed limitations at urban intersections, the velocity range is from 0 to 3 cells/s on the major road and 0 to 2 cells/s on the minor road. The maximum acceleration and deceleration in physical units are set to  $4 \text{ m/s}^2$  and  $8 \text{ m/s}^2$ , respectively. One time step corresponds to 1 s. In addition, vehicle overtaking is not considered in the simulation. The signal cycle of the selected intersection is also employed in the two cellular automata models. The signal cycle will run continuously throughout the simulation to better observe vehicle delays.

By inputting different traffic volumes, the VISSIM models and the cellular automata models are executed simultaneously several times. Finally, we can compare the average vehicle delays produced by these models to determine the effectiveness of the cellular automata model for MUT intersections.

### 5.3. Simulation Result Analysis

There is no doubt that the intersection channelization information, traffic volume information, and signal timing collectively affect the operational performance of MUT intersections. Table 6 shows the simulation results of the cellular automata model and VISSIM model over five consecutive days.

It can be seen from Table 6 that, compared to the current MUT intersection, the modified MUT intersection reduces the average vehicle delay to varying degrees (regardless of which simulation model is used). For the simulation results of the VISSIM models, the percentage reductions in the average vehicle delay are 10.1%, 14.1%, 13.5%, 12.6%, and 10.7% from Day 1 to Day 5, respectively. For the simulation results of the cellular automata models, the percentage reductions in the average vehicle delay are 11.3%, 13.6%, 13.7%, 12.7%, and 9.8% from Day 1 to Day 5, respectively.

It is worth noting that modeling uncrossable boundaries with a certain width in cellular automata models has still not been fully explored in relevant theoretical frameworks and the literature. Due to this limitation, we simplified the cellular automata model by not accounting for the width of the median U-turn. This simplification may have contributed to the worse simulation results of the cellular automata models compared to the VISSIM models (regardless of whether the current or modified MUT intersection is considered).

However, the discrepancy between the average vehicle delay results of the cellular automata models and VISSIM models are relatively low, with the maximum error being around 7%.

**Table 6.** The simulation results of the cellular automata model and VISSIM model.

Comparison		Day 1		Day 2		Day 3		Day 4		Day 5	
		SV	CV								
Current MUT intersection	Average vehicle delay	51.3	48.5	56.6	52.8	57.2	53.6	52.2	49.5	54.2	51.3
	Error	5.5%		6.7%		6.3%		5.2%		5.4%	
Modified MUT intersection	Average vehicle delay	46.1	42.9	48.6	45.3	49.4	46.1	45.6	42.9	48.4	46.2
	Error	6.9%		6.8%		6.7%		5.9%		4.5%	

SV indicates the simulation result of VISSIM; CV indicates the simulation result of cellular automata. Error =  $(SV - CV)/SV \cdot 100\%$ .

Based on the analysis above, the comparisons confirm that the proposed cellular automata model demonstrates relatively high accuracy when calculating the average vehicle delay for the selected MUT intersection. Furthermore, it can be shown that the proposed cellular automata model effectively reflects vehicle movements at the selected MUT intersection. Additionally, the simulation results of the modified MUT intersection indicate that the proposed calculation methods for critical parameters of MUT intersections can be beneficial for reducing average vehicle delay.

### 6. Sensitivity Analysis

Average vehicle delay is influenced by several factors, including the separation distance, the gap of the median U-turn, the proportion of left-turn vehicles, and the green phase percentage, among others. To further evaluate the operational performance of the modified MUT intersection under various influencing factors, this section will systematically conduct sensitivity experiments to explore how these factors impact the average vehicle delay at the intersection. Under the same conditions, the average vehicle delay of the current MUT intersection will serve as the control group. Field data representing the highest traffic volume will be used as inputs for the proposed cellular automata model in the simulation. Details of the experiments analyzing the percentage reduction in average vehicle delay for the modified MUT intersection are provided in the following subsections.

#### 6.1. Effect of the Separation Distance and the Gap of the Median U-Turn on Average Vehicle Delay

As two important elements in MUT intersection design, the separation distance and the gap of the median U-turn have a significant effect on the operational performance of MUT intersections. In this subsection, different combinations of separation distance and gap of the median U-turn will be analyzed to examine their effects on delay reduction. The gap of the median U-turn is set to 4 m, 6 m, 8 m, 10 m, and 12 m. The separation distance on the east and west sides of the modified MUT intersection is set to 108 m, 112 m, 116 m, 120 m, 124 m, 128 m, 132 m, 136 m, 140 m, and 144 m, and 72 m, 76 m, 80 m, 84 m, 88 m, 92 m, 96 m, 100 m, 104 m, and 108 m, respectively. The remaining settings for the simulation experiments remain unchanged. Figure 11 illustrates the delay reductions for different combinations of the separation distance on the east and west sides of the modified MUT intersection and the gap of the median U-turn.

As shown in Figure 11, when the separation distance on the east and west sides of the modified MUT intersection is certain, increasing the gap of the median U-turn results in only a limited improvement in delay reduction. Only a small portion of the results indicate continued growth in delay reduction. It is considered that appropriately widening the gap of the median U-turn can help reduce average vehicle delay to some extent. However, an excessive gap at the median U-turn allows multiple left-turn vehicles from either the

major or minor road to turn around simultaneously. This can more severely disrupt the normal driving of the straight-through vehicles on the major road and lead to increased average vehicle delays. Therefore, the benefit of delay reduction will decrease under certain conditions. Overall, it can be said that the effects of the gap of the median U-turn on the operational performance of MUT intersections are quite limited.

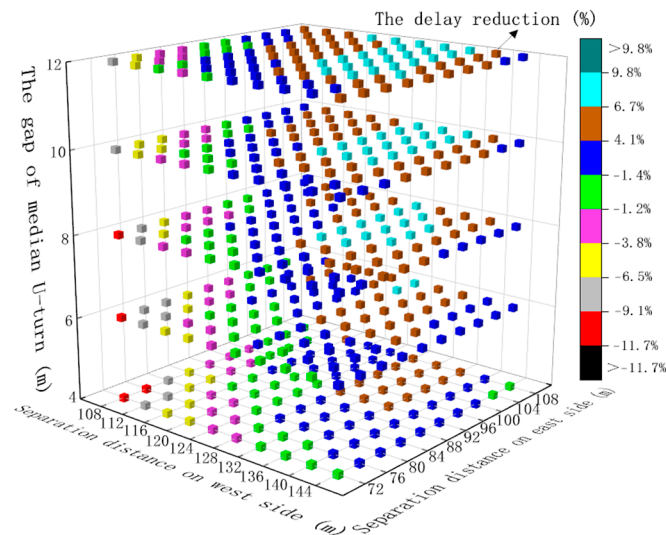


**Figure 11.** Vehicle delay reduction for different gaps at median U-turns and separation distances.

When we consider the separation distance on the west (or east) side of the modified MUT intersection and the gap of the median U-turn as reference coordinates, it can be observed that increasing the separation distance on the opposite side leads to a corresponding reduction in average vehicle delay. However, as the separation distance on both sides continues to increase, the degree of delay reduction begins to stabilize or even decline. This phenomenon can be attributed to the reason that, when the separation distance on both sides of the modified MUT intersection is sufficiently long, left-turn vehicles will have more queuing space outside the median U-turn. The probability of congestion at the intersection will be reduced to a certain degree. In addition, a longer separation distance allows the intersection to accommodate more traffic flow while minimizing the impact of left-turn traffic on through traffic. However, an excessively long separation distance may increase complexity in traffic environments. Left-turn vehicles must drive a longer distance to detour around the intersection, which increases the travel time. Drivers may misjudge the traffic conditions at the intersection, which can lead to unsafe driving decisions. Moreover, when left-turn traffic weaves with through traffic, it increases the risk of confusion and congestion, which can contribute to increased average vehicle delay. Therefore, in practice, the traffic departments need to carefully balance the separation distances and the gap in the median U-turn to optimize the operational performance of MUT intersections.

### 6.2. Effect of the Vehicle Free-Flow Speed and the Proportion of Left-Turn Vehicles in Corresponding Road Traffic Volume on Average Vehicle Delay

The vehicle free-flow speed and the proportions of left-turn vehicles on both the major and minor roads may critically influence the delay reduction at the modified MUT intersection. In this subsection, the proportions of left-turn vehicles on the major and minor roads are set between 0.1 and 0.9. The vehicle free-flow speed is set between 2 m/s to 11 m/s. All other simulation parameters remain unchanged. Next, the impact of these factors on delay reduction will be analyzed. Figure 12 presents the delay reduction for various combinations of left-turn vehicle numbers on major and minor roads and vehicle free-flow speeds.

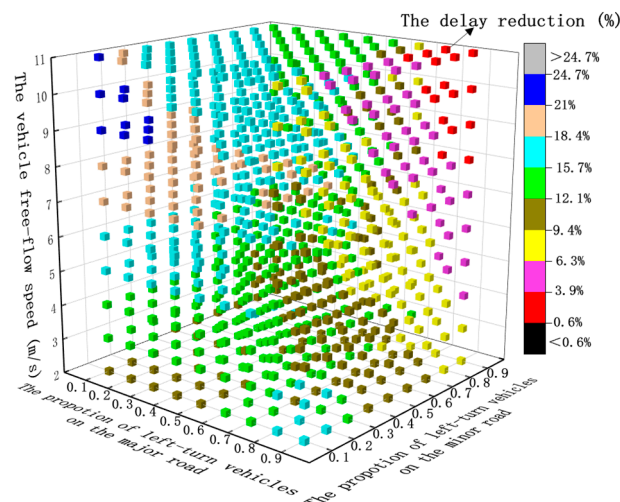


**Figure 12.** Vehicle delay reduction for different vehicle free-flow speeds and numbers of left-turn vehicles.

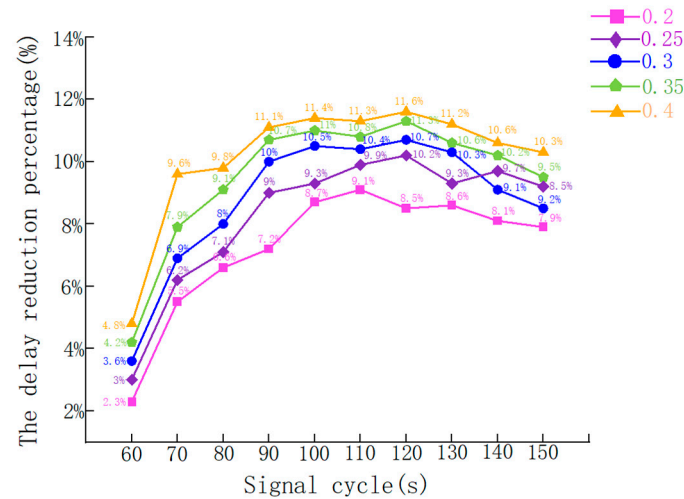
As shown in Figure 12, when the proportion of left-turn vehicles on both the major and minor roads is at its minimum, increasing the vehicle free-flow speed leads to an improvement in delay reduction. Subsequently, as the proportion of left-turn vehicles on the major and minor roads continues to increase, delay reduction initially increases accordingly with a higher vehicle free-flow speed, but then begins to decrease. When the proportion of left-turn vehicles on the major and minor roads becomes sufficiently large, further increases in the vehicle free-flow speed cause the delay reduction to decrease steadily. Appropriately increasing the vehicle free-flow speed can help dissipate queuing vehicles and reduce average vehicle delays to some extent. However, an excessively high vehicle free-flow speed means that more vehicles will pass through the intersection during a green phase. This can result in the excessive queuing of left-turn vehicles outside the median U-turn, which may not dissipate in time. In addition, drivers may need to spend more time avoiding fast-moving vehicles while turning around. Consequently, the degree of delay reduction will decrease.

Figure 12 also demonstrates that, at low vehicle free-flow speeds (2 m/s to 3 m/s) and low proportions of left-turn vehicles on both the major and minor roads (0.1 to 0.3), there is a significant increase in delay reduction. Under normal traffic conditions, MUT intersections are generally considered effective for enhancing the operational performance of urban intersections when either the major or minor road has a high proportion of left-turn vehicles. However, in most cases, the proportion of left-turn vehicles on both roads is negatively correlated with delay reduction. The higher the proportion of left-turn vehicles, the less significant the degree of delay reduction becomes. This phenomenon is commonly observed at different vehicle free-flow speeds. The possible reason is that an excess of left-turn vehicles may cause blockages and overflow at median U-turns, further disrupting the normal traveling of traffic on the major road. This ultimately leads to a decline in the overall traffic efficiency of the intersection. Therefore, it is particularly important to effectively coordinate the relationship between the proportion of left-turn vehicles and vehicle free-flow speed in urban traffic management.

### 6.3. Effects of Green Phase Percentage and Signal Cycle on Average Vehicle Delay

In this subsection, we analyze the delay reduction in the modified MUT intersection under different green phase percentages and signal cycle durations. In typical traffic environments, major roads usually experience higher traffic volumes. Consequently, the settings of the green phase percentage for the major road significantly affect the overall performance of intersections. The delay reduction degree can be observed directly by varying the green phase percentage. Therefore, the percentage of the green phase of the major road is set to 0.2, 0.25, 0.3, 0.35, and 0.4. The traffic signal cycle durations range from

60 s to 150 s. The proportion of left-turn vehicles is fixed at 1:3. The vehicle lane change rate is set at 0.7, and the probability of vehicle random slowing is 0.5. The free flow speed is set to 8 m/s. All other parameters of the cellular automata models remain unchanged. The delay reduction results are shown in Figure 13.



**Figure 13.** Vehicle delay reduction for different green time percentages and signal cycle durations.

As shown in Figure 13, when the signal cycle is certain, the degree of delay reduction increases with the increase in the green timing percentage. This is because a higher green phase percentage allows more left-turn and straight-through vehicles on the major road to pass through the intersection, which helps dissipate queuing vehicles more quickly and reduces vehicle queuing time. As a result, the degree of delay reduction will be greater. When the green phase percentage of the major road is certain, the degree of delay reduction increases continuously from 60 s to 120 s. However, the delay reduction gradually decreases from 130 s to 150 s. This indicates that appropriately increasing the signal cycle and green phase duration within a specific range is beneficial for improving the traffic efficiency of MUT intersections. However, as the signal cycle and green phase duration continue to increase, the number of vehicles passing through the intersection during the corresponding time will also rise. This may cause drivers of left-turn and right-turn vehicles on the minor road to make more cautious decisions when weaving with the vehicles from the major road. Additionally, excessive vehicles on the major road may form a sufficiently long queue outside the median U-turn. These situations can lead to an increase in delay times. The delay reduction will decrease during a specific signal cycle and duration of the green phase time.

## 7. Comparative Discussion of Proposed Findings and Relevant Case Studies

To more effectively evaluate the similarities and differences in the performance of MUT intersections across various regions and traffic environments, this study compares its findings with those from similar case studies, specifically focusing on RCUT and DLT intersection designs. By examining these different intersection types, we can highlight the varying impacts on operational efficiency, safety, and congestion. This comparative analysis provides valuable insights into the effectiveness of MUT intersections relative to other designs.

### 7.1. Comparison of Intersection Operations

MUT, RCUT, and DLT intersections are designed to address the challenges caused by left-turn movements at conventional intersections, which frequently lead to traffic congestion and safety risks. However, each design employs a different approach to achieve this objective. For the MUT design, it works by rerouting left-turning vehicles through a median U-turn instead of allowing direct left turns at the intersection. This design eliminates

left-turn conflicts with through traffic. Findings from this study indicate that MUT intersections significantly reduce the number of conflict points and improve operational efficiency by decreasing vehicle delays. The field data collected from a MUT intersection in Xi'an, China, confirm that the MUT design effectively addresses congestion issues and enhances the safety performance of the intersection. With regard to the RCUT design, it reduces left-turn conflicts by requiring left-turning vehicles to perform a U-turn at a specific location rather than directly at the intersection. Although the RCUT design does not eliminate all left-turn movements, it can reduce congestion at the intersection. According to Raunak et al., RCUT intersections are effective in reducing accidents and improving traffic flow, particularly by reducing left-turn and head-on collisions [49]. Jonathan et al. further emphasize that RCUT intersections can reduce crash rates by up to 50% compared to conventional intersections [50]. Lastly, the DLT design redirects left-turn lanes away from the intersection to a position either before or after the main intersection. DLT allows left-turning vehicles to bypass the intersection, reducing conflicts between left-turning vehicles and through traffic. Research conducted by Ahmed et al. and Zhao et al. suggests that DLT intersections can effectively reduce delays and improve safety by separating left-turn movements from through traffic [51,52]. However, while the DLT design improves operational efficiency by reducing direct conflicts, it does not fully resolve the potential for congestion caused by the remaining left-turn traffic. In comparison, MUT intersections have the advantage of completely eliminating left-turn movements, resulting in a potentially greater reduction in conflict points and accidents.

### 7.2. Comparison of Operational Efficiency and Safety

MUT, RCUT, and DLT designs exhibit distinct advantages and limitations regarding intersection safety and capacity. The MUT design, in particular, is highly effective in improving traffic flow and safety at high-volume intersections. The findings from this study support these conclusions, particularly in complex urban environments. The simulation results from the cellular automata model used in this study align with previous studies that show a remarkable improvement in the operational performance and safety of MUT intersections.

RCUT intersections also improve operational efficiency by minimizing left-turn congestion. However, RCUTs do not completely eliminate left-turn traffic; instead, they redirect it to a secondary U-turn location. While this strategy reduces direct left-turn conflicts, it may still result in some delays for left-turn vehicles, especially during peak traffic periods. According to the Federal Highway Administration (FHWA), RCUTs can achieve a 25–45% reduction in crash rates [53]. Molan et al. found that RCUT intersections improved intersection safety by more than 30% by reducing the likelihood of left-turn accidents [54]. However, RCUT intersections may experience higher delay times than MUT intersections due to the need for vehicles to perform a U-turn at a distant location.

DLT intersections, by relocating left-turn lanes away from the intersection, reduce delays and congestion associated with left-turning vehicles. Zhang et al. and Qu et al. conclude that DLT intersections can provide significant safety and traffic efficiency improvements [55,56]. However, DLT does not fully address the potential for congestion caused by the remaining left-turn traffic, which may still conflict with other movements in the modified left-turn lanes.

Overall, the MUT design stands out as the most effective in improving both traffic flow and safety, particularly at high-volume intersections, by completely eliminating left-turn movements and significantly reducing conflict points.

## 8. Conclusions

This paper proposes theories for determining the critical parameters of MUT intersections. It also presents a delay model of MUT intersections based on vehicle dynamic operations. Vehicle average delay is chosen as the evaluation index. We analyzed which possible factors can impact the performance of MUT intersections, such as the separation

distance, the gap of the median U-turn, the proportion of left-turn vehicles, and green phase percentage, etc. Based on the results of the simulation experiments, the following conclusions can be drawn:

1. The critical parameters of MUT intersections can be concluded as one of the important factors affecting vehicle average delay.
2. Compared to the VISSIM model, the proposed cellular automata model demonstrates relatively high accuracy, with the errors around 7%.
3. Compared to the current intersection, the modified intersection performs better in reducing vehicle average delays in various conditions.

The established framework offers a systematic analytical method to better obtain a series of operational performance metrics for MUT intersections. Additionally, this framework also helps us understand the dynamic variation in vehicle average delay under different simulation parameters for further exploring MUT intersections. Additionally, we conduct a stakeholder analysis to enhance the practical application and value of this study's findings. The major stakeholders include traffic control operators, local authorities, and road safety authorities. For traffic control operators, the proposed delay model provides a valuable tool for optimizing signal timing at MUT intersections, improving traffic flow and reducing delays, which facilitates more efficient road use and congestion management. Local authorities and transportation planners can use the study's insights to inform the design and upgrading of MUT intersections, incorporating the model's critical parameters to address varying traffic volumes and operational needs, leading to more efficient transportation networks. Moreover, road safety authorities can apply the delay model to assess the safety and efficiency of MUT intersections, contributing to improved road safety and reducing accidents. Based on these considerations, it is recommended that these stakeholders integrate the delay model and its parameters into intersection design and modification processes to optimize traffic performance, promote safety, and improve the overall transportation system.

However, it is worth noting that the proposed cellular automata model still has some limitations. For instance, we do not take into account the impact of the width of the median U-turn on the performance of MUT intersections. Moreover, under a uniform vehicle arrival rate at each entrance, the proposed cellular automata model may still perform well enough in different simulation environments. Future research should explore several areas as follows. First, the impact of the median U-turn width on intersection performance should be explored because this factor can enhance predictive accuracy, especially for intersections with varying U-turn designs. Additionally, the model's assumption of uniform vehicle arrival rates should be revised to account for non-uniform traffic flow, which would improve its robustness and applicability. Finally, extending the model to other intersection types, such as signalized intersections and roundabouts, would help evaluate the broader applicability of the proposed framework. These improvements would enhance the model's versatility and accuracy, making it a more effective instrument for traffic management in diverse environments.

We will consider more relevant factors to further improve the accuracy and applicability of the proposed cellular automata model.

**Author Contributions:** Conceptualization, X.L. and W.Z.; methodology, C.Z. and X.L.; writing—original draft preparation, C.Z. and T.W.; investigation, C.Z. and T.W.; writing—review and editing, X.L. and W.Z. All authors have read and agreed to the published version of the manuscript.

**Funding:** This paper was supported by the China Postdoctoral Science Foundation (No. 2022M711806). The authors would like to thank [China Postdoctoral Science Foundation] for their financial support.

**Institutional Review Board Statement:** Not applicable.

**Informed Consent Statement:** Not applicable.

**Data Availability Statement:** No new data were created or analyzed in this study. Data sharing is not applicable to this article.

**Acknowledgments:** Thanks to the support from the China Postdoctoral Science Foundation (No. 2022M711806) and the colleagues in this group dealing with the large amount of data.

**Conflicts of Interest:** The authors declare no conflict of interest.

## References

1. Fu, D.J.; Zhang, C.B.; Liu, J.; Li, T.; Li, Q.L. Research of the left-turn vehicles lane-changing behaviors at signalized intersections with contraflow lane. *Phys. A* **2024**, *633*, 129364. [CrossRef]
2. Anciaes, P.; Nascimento, J.M. Road traffic reduces pedestrian accessibility—Quantifying the size and distribution of barrier effects in an African city. *J. Transp. Health* **2022**, *27*, 101522. [CrossRef]
3. Wang, X.S.; Mohamed, A.A. Modeling left-turn crash occurrence at signalized intersections by conflicting patterns. *Accid. Anal. Prev.* **2008**, *40*, 76–88. [CrossRef] [PubMed]
4. Zhao, J.; Liu, Y. Safety evaluation of intersections with dynamic use of exit-lanes for left-turn using field data. *Accid. Anal. Prev.* **2017**, *102*, 31–40. [CrossRef]
5. Juteak, O.; Eungcheol, K.; Myungseob, K.; Sangho, C. Development of conflict techniques for left-turn and cross-traffic at protected left-turn signalized intersections. *Saf. Sci.* **2010**, *48*, 460–468.
6. Ni, Y.; Wang, M.L.; Sun, J.; Li, K. Evaluation of pedestrian safety at intersections: A theoretical framework based on pedestrian-vehicle interaction patterns. *Accid. Anal. Prev.* **2016**, *96*, 118–129. [CrossRef]
7. Zhao, J.; Victor, L.K.; Wang, M. Two-dimensional vehicular movement modelling at intersections based on optimal control. *Transp. Res. Part B Methodol.* **2020**, *138*, 1–22. [CrossRef]
8. Liu, H.; Vikash, V.G. A novel Max Pressure algorithm based on traffic delay. *Transp. Res. Part C Emerg. Technol.* **2022**, *143*, 103803. [CrossRef]
9. Federal Highway Administration. Signalized Intersection. Available online: <https://safety.fhwa.dot.gov/intersection/signal/index.cfm> (accessed on 12 March 2021).
10. Kay, J.; Gates, T.J.; Savolainen, P.T.; Shakir, M.M. Safety performance of unsignalized median U-turn intersections. *Transp. Res. Rec.* **2020**, *2676*, 451–466. [CrossRef]
11. Ma, Z.; Xie, J.; Qi, X.; Xu, Y.; Sun, J. Two-dimensional simulation of turning behavior in potential conflict area of mixed-flow intersections. *Comput. Aided Civ. Infrastruct. Eng.* **2017**, *32*, 412–428. [CrossRef]
12. Federal Highway Administration. *Improving Intersections for Pedestrians and Bicyclists*; FHWA-SA-22-017; Federal Highway Administration: Washington, DC, USA, 2022.
13. Federal Highway Administration. *Median U-Turn Intersection*; FHWA-HRT-092-057; Federal Highway Administration: Washington, DC, USA, 2009.
14. Al-Omari, M.M.; Abdel, A.M.; Lee, J.; Yue, L.; Abdelrahman, A. Safety Evaluation of Median U-Turn Crossover-Based Intersections. *Transp. Res. Rec.* **2020**, *2674*, 206–218. [CrossRef]
15. Federal Highway Administration. *Alternative Intersections/Interchanges: Informational Report (AIIR)*; FHWA-HRT-09-060; Federal Highway Administration: Washington, DC, USA, 2009.
16. Hummer, J.E.; Reid, J.D. *Unconventional Left-Turn Alternatives for Urban and Suburban Arterials—An Update*; No. E-C019; Urban Street Symposium: Dallas, TX, USA, 2007.
17. Maryam, M.S.; Dixon, K.K.; Fitzpatrick, K. Determining variables that influence the operation and safety of median openings in close proximity to signalized intersections. *Transp. Res. Rec.* **2022**, *2676*, 1–12. [CrossRef]
18. Liu, P.; Lu, J.J.; Chen, H. Safety effects of the separation distances between driveway exits and downstream U-turn locations. *Accid. Anal. Prev.* **2008**, *40*, 760–767. [CrossRef] [PubMed]
19. Zhou, H.; Hsu, P.; Lu, J. Optimal location of U-turn median openings on roadways. *Trans. Res. Rec.* **2003**, *1847*, 36–41. [CrossRef]
20. Jing, D.f.; Song, C.C.; Guo, Z.Y.; Li, R. Influence of the median opening length on driving behaviors in the crossover work zone—A driving simulation study. *Transp. Res. Part F Traffic Psychol. Behav.* **2021**, *82*, 333–347.
21. Jagannathan, R. *Synthesis of the Median U-Turn Intersection Treatment, Safety, and Operational Benefits* (No. FHWA-HRT-07-033); Federal Highway Administration: Washington, DC, USA, 2007.
22. Mane, A.S.; Pulugurtha, S.S. Applicability of Unconventional Intersection Designs Over Pretimed Signalized Intersection Design Along a Coordinated Corridor. *Trans. Res.* **2020**, *45*, 503–516.
23. Al-Omari, M.M. Evaluation of Unconventional Signalized Intersections on Arterial Roads and a Proposition for a Novel Intersection Design. Ph.D. Thesis, University of Central Florida, Orlando, FL, USA, 2020; p. 1316.
24. Liu, Z.; Bie, Y. Comparison of hook-turn scheme with U-turn scheme based on actuated traffic control algorithm. *Transp. A Transp. Sci.* **2015**, *11*, 484–501. [CrossRef]
25. Liu, P.; Qu, X.; Yu, H.; Wang, W.; Cao, B. Development of a VISSIM simulation model for U-turns at unsignalized intersections. *J. Transp. Eng.* **2012**, *138*, 1333–1339. [CrossRef]
26. Mazaheri, A.; Amir, M.R. Determining a suitable position for U-turns near signal-controlled road junctions. *Proc. Inst. Civ. Eng. Transp.* **2017**, *170*, 267–275. [CrossRef]
27. El, E.M.; Sayed, T. Operational performance analysis of the unconventional median U-turn intersection design. *Can. J. Civ. Eng.* **2011**, *38*, 1249–1261.

28. Taberbero, V.; Sayed, T. Upstream signalized crossover intersection: An unconventional intersection scheme. *J. Transp. Eng.* **2006**, *132*, 907–911. [[CrossRef](#)]
29. Schultz, G.G.; Allen, C.G.; Boschert, T. Making the most of an existing system through access management at major arterial intersections. *Trans. Res. Rec.* **2010**, *2171*, 66–74. [[CrossRef](#)]
30. Transportation Research Board. *Highway Capacity Manual (HCM 2010)*; National Academics: Washington, DC, USA, 2010.
31. Liu, R.W. Queuing model for U-turn mouth of bi-directional streets. *J. Chongqing Jingtong Univ. Nat. Sci. Ed.* **2009**, *28*, 921–925. (In Chinese)
32. Khan, T.; Vivek, A.K.; Mohapatra, S.S. Comparative appraisal of critical gap estimation techniques in the context of U-turning vehicles. *Trans. Res. Rec.* **2021**, *2675*, 1408–1421. [[CrossRef](#)]
33. Emily, N.; Lam, A.M.; Wassim, N. Naturalistic Study of Truck Following Behavior. *Trans. Res. Rec.* **2017**, *2615*, 35–42.
34. Federal Highway Administration. *Manual on Uniform Traffic Control Devices*; Federal Highway Administration: Washington, DC, USA, 2009.
35. Federal Highway Administration. *Intersection Safety: A Manual for Local Rural Road Owners*; Federal Highway Administration: Washington, DC, USA, 2011.
36. Qin, Y.Y. Modeling the mixed traffic capacity of minor roads at a priority intersection. *Phys. A* **2024**, *636*, 129541. [[CrossRef](#)]
37. Lee, J.Y.; Lee, E.; Lee, S.; Kim, T.; Son, B. Estimating the Effects of Freeway Weaving Section Length on Level of Service Based on Microsimulation. *Trans. Res. Rec.* **2023**, *2677*, 205–218. [[CrossRef](#)]
38. Transportation Research Board. *Highway Capacity Manual (HCM 2000)*; National Academics: Washington, DC, USA, 2000.
39. Federal Highway Administration. *Preferred Following Distance as a Function of Speed—Function Specific Automation (Level 1) Applications*; Federal Highway Administration: Washington, DC, USA, 2021.
40. American Association of Motor Vehicle Administrators. *Model Commercial Driver License Manual*; AAMVA: Arlington, VA, USA, 2014; Section 2.7.
41. Jessica, S.J. Crash avoidance potential of four large truck technologies. *Accid. Anal. Prev.* **2012**, *49*, 338–346.
42. Wael, K.M.; Miho, A.; Hideki, N.; Dang, M.T. Stochastic approach for modeling the effects of intersection geometry on turning vehicle paths. *Transp. Res. Part C Emerg. Technol.* **2013**, *32*, 179–192.
43. Chen, P.; Zeng, W.L.; Yu, G.Z. Assessing right-turning vehicle-pedestrian conflicts at intersections using an integrated microscopic simulation model. *Accid. Anal. Prev.* **2019**, *129*, 211–224. [[CrossRef](#)] [[PubMed](#)]
44. Li, X.; Sun, J.Q. Effects of turning and through lane sharing on traffic performance at intersections. *Phys. A* **2016**, *444*, 622–640. [[CrossRef](#)]
45. Liang, S.D. Signalized intersection dynamic straight-right lane design and evaluation. *Phys. A* **2023**, *620*, 128771. [[CrossRef](#)]
46. Yang, Q.L.; He, Y.Z. Right-turn-on-red queueing process at signalized intersections with a short right-turn lane. *Phys. A* **2022**, *598*, 127395. [[CrossRef](#)]
47. Yang, Q.L.; Fu, X. An extended queueing model for vehicles at signalized intersections considering the platoon correlated arrivals. *Phys. A* **2024**, *635*, 129483. [[CrossRef](#)]
48. Planning Transport Verkehr AG (PTV). *VISSIM, 4.0*. Computer Software. PTV Group: Karlsruhe, Germany, 2010.
49. Raunak, M.; Srinivas, S.P. Safety evaluation of unsignalized and signalized restricted crossing U-turn (RCUT) intersections in rural and suburban areas based on prior control type. *IATSS Res.* **2022**, *46*, 247–257.
50. Jonathan, H.; Amirarsalan, M.M.; Xu, S.Q. Modeling the performance of restricted crossing U-turn intersections including the effects of connected and autonomous vehicles: A case study in California. *Can. J. Civ. Eng.* **2023**, *50*, 560–570.
51. Ahmed, A.; Mohamed, A.; Jaeyoung, L. Evaluation of displaced left-turn intersections. *Transp. Eng.* **2020**, *1*, 100006.
52. Zhao, J.; Ma, W.J. Optimal operation of displaced left-turn intersections: A lane-based approach. *Transp. Res. Part C* **2015**, *61*, 29–48. [[CrossRef](#)]
53. Federal Highway Administration. *Field Evaluation of a Restricted Crossing U-Turn Intersection*; FHWA-HRT-11-067; Federal Highway Administration: Washington, DC, USA, 2012.
54. Molan, A.M.; Howard, J.; Islam, M. A framework for estimating future traffic operation and safety performance of restricted crossing U-turn (RCUT) intersections. *Open Transp. J.* **2022**, *16*, 1. [[CrossRef](#)]
55. Zhang, X.C.; Gao, S. Signal control method and performance evaluation of an improved displaced left-turn intersection design in unsaturated traffic conditions. *Transp. Met. B Transp. Dyn.* **2020**, *1*, 8.
56. Qu, W.; Sun, Q.; Zhao, Q.; Tao, T.; Qi, Y. Statistical Analysis of Safety Performance of Displaced Left-Turn Intersections: Case Studies in San Marcos, Texas. *Int. J. Environ. Res. Public Health* **2020**, *17*, 6446. [[CrossRef](#)] [[PubMed](#)]

**Disclaimer/Publisher’s Note:** The statements, opinions and data contained in all publications are solely those of the individual author(s) and contributor(s) and not of MDPI and/or the editor(s). MDPI and/or the editor(s) disclaim responsibility for any injury to people or property resulting from any ideas, methods, instructions or products referred to in the content.